Pakistan Veterinary Journal

ISSN: 0253-8318 (PRINT), 2074-7764 (ONLINE)
DOI: 10.29261/pakvetj/2025.211

RESEARCH ARTICLE

Tupistra chinensis Polysaccharide Mitigates the Inflammatory Response by Regulating Gut-Microbiota in Mice Induced by LPS

Xiaohui Liang[1,2*], Jiadong Chen[3], Chang Xu[3], Qing He[3], Munawar Ali[3] and Kun Li[3*]

[1]School of Life Sciences, Qilu Normal University, Jinan 250200, PR China; [2]Energy Research Institute, Qilu University of Technology (Shandong Academy of Sciences), Jinan 250014, PR China; [3]College of Veterinary Medicine, Nanjing Agricultural University, Nanjing 210095, China.

*Corresponding author: liang0168@foxmail.com; lk3005@njau.edu.cn

ARTICLE HISTORY (25-505)

Received: May 06, 2025
Revised: July 27, 2025
Accepted: July 29, 2025
Published online: August 11, 2025

Key words:
Gut microbiota
Inflammatory bowel disease
Lipopolysaccharides
Mice
Tupistra chinensis
polysaccharide

ABSTRACT

Tupistra chinensis polysaccharide (TCP), also known as "kaikoujian" in Chinese, is used to treat illnesses including rheumatic diseases, snake bites, and inflammation. Its impacts on microbiota and immunity were unclear. We studied TCP's ability to mitigate LPS-induced inflammatory intestinal damage in mice. ICR mice (n=30) were divided equally into: Control (C), LPS-induced model (M), and TCP-treated (P) groups. The P group received TCP (100 mg/kg) daily for 14 days. On the 14th day, mice in the M and P groups were given 10 mg/kg LPS by intraperitoneal injection. The results indicate that LPS causes obvious inflammation and reduced antioxidant capacity in the intestinal epithelium of mice. Additionally, the LPS-challenged group exhibited reduced intestinal microbial diversity and induced apparent structural changes, as evidenced by a significant increase in the richness of harmful bacteria (*Duncaniella*, *Eubacterium,* and *Paramuribaculum*). In contrast, the abundance of beneficial bacteria (*Phocaeicola*, *Bacteroides,* and *Muribaculaceae*) was notably decreased. Notably, TCP treatment significantly modulates gut microbiota to reduce the inflammatory response and oxidative damage by lowering the inflammatory cytokines (IL-1β, IL-6, IL-10, TNF-α) and regulating the antioxidant parameters (T-AOC, GSH-Px, SOD, MDA) induced by LPS in mice. Conclusively, our findings demonstrated that TCP treatment protects the intestinal epithelium against LPS-induced inflammatory response and gut microbiota disorders. These novel findings provide a basis for future research on the therapeutic potential of TCP in mitigating LPS-induced damage in humans and animals.

To Cite This Article: Liang X, Chen J, Xu C, He Q, Ali M, and Li K 2025. *Tupistra chinensis* polysaccharide mitigates the inflammatory response by regulating gut-microbiota in mice induced by LPS. Pak Vet J. http://dx.doi.org/10.29261/pakvetj/2025.211

INTRODUCTION

Tupistra chinensis (TC), also called "kaikoujian" in Chinese, is used to cure many conditions, including rheumatic diseases, snake bites, and inflammations (Pan *et al.*, 2012). *Tupistra chinensis* grows in southwest China and has dry roots that are used as a folk medicine in the Shennongjia Forestry District, a National Nature Reserve in Hubei (Zhou *et al.,* 2024). The main active components in TC contain steroidal saponins, polysaccharides, and aliphatic acid (Li *et al.*, 2015; Song *et al.*, 2021). Research has shown that TC saponins can induce cancer cell apoptosis and exert anti-inflammatory effects by inhibiting NO production induced by LPS, while TC polysaccharide (TCP) has anti-inflammatory and antioxidant activities, with few adverse effects (Wang *et al.*, 2020b; Xu *et al.*, 2020). Interferons are potent antiviral agents against viral diseases in different species (Anjum *et al*., 2020). However, research about the anti-inflammatory mechanism of TCP is still lacking.

The gut microbiota inhabiting the host's gastrointestinal tract acts as a dynamic "hidden organ," essential for numerous defense mechanisms and critical physiological functions during both health and disease (Kesika *et al.,* 2021). This complex community comprises trillions of microorganisms, vastly outnumbering human cells (Marchesi *et al.*, 2016; Fan and Pedersen, 2021). Research consistently demonstrates its diverse roles, including regulating immune responses, managing metabolism, and maintaining microenvironmental balance (Wilson and

Nicholson, 2017). The microbiota exerts its influence through multiple pathways: directly eliminating competing bacteria, generating inhibitory metabolites including short-chain fatty acids (SCFA) and bile acids (BA), and competing for space and nutrients (Buffie *et al.*, 2015; Sassone-Corsi *et al.*, 2016). Alterations in microbiota composition or breaches in the intestinal barrier depend on various conditions, including inflammatory bowel disease, colorectal cancer, and type 2 diabetes (Zhang *et al.*, 2020; Hong *et al.*, 2022; Song *et al.*, 2023). Several recent studies have employed LPS to generate IBD models and achieved promising outcomes (Qian *et al.*, 2020). Limited information exists regarding the effects of TCP on LPS-induced gut microbiota dysbiosis in mice. To address this, we examined TCP's potential to mitigate immune dysfunction caused by lipopolysaccharides (LPS) in mice. Using an LPS-induced inflammation model, we evaluated TCP's effects by measuring inflammatory factor levels and sequencing gut microbiota. This study may provide evidence that TCP can be used to protect gut-intestinal health.

MATERIALS AND METHODS

Extraction of *Tupistra chinensis* polysaccharides*:* The extraction was conducted following the previously published method for similar herbs (Wang *et al.*, 2020a). Briefly, Rhizomes of TC (50.0 kg) were washed, chopped, and degreased with 95% ethanol thrice at 65°C. The remaining residue underwent hot water extraction three times, then the extract was concentrated and dried to obtain crude polysaccharide. After dialysis and depigmentation, the tube's lower layer was collected as TCP for further use. To determine the concentration of polysaccharides, we employed the phenol sulfuric acid method.

Animal, experiment design: Thirty (n=30) ICR mice were procured from Yangzhou University, China. After a week of adaptation period, mice were equally (n=10) distributed into three groups: Control group (C), an LPS-inducing group (M), and TCP treatment group (P). The experimental protocol was permitted by the Ethics Committee of Nanjing Agricultural University (NJAU.No20240226021). During 14 days of treatment, the P group was given 100 mg/kg TCP (Huang, 2013; Rai *et al.,* 2024), the C group and M group mice were given sterile water in the same volume. All mice were weighed daily. On the 14th day, mice in the M and P groups were given 10 mg/kg LPS by intraperitoneal injection. The dose of LPS challenge was referenced from a similar study (He *et al.*, 2023). The next day, all mice were euthanized under anesthesia to collect blood, spleen, and colon contents. The spleen was weighed to calculate organ index, blood was kept at 4°C, and colon contents were kept at -80°C for further use.

Serum antioxidants and cytokine analysis: After anesthetization, blood was collected in tubes by retro-orbital puncture. The serum was separated following centrifugation at 4000×g for 15 minutes and then kept at −80°C until further use. The concentrations of malondialdehyde (MDA), superoxide dismutase (SOD), total antioxidant capacity (T-AOC), and glutathione peroxidase (GSH-Px) were detected by commercially available kits. Cytokine levels, including interleukin 6 (IL-6), IL-1β, IL-10, and tumor necrosis factor (TNF-α), were quantified using commercial detection kits.

Genomic DNA extraction: The DNA from mice's colon guts was obtained by using the DNA stool kit (Qiagen, USA). After that, DNA was quantified by UV-vis spectrophotometer (NanoDrop 2000, Thermo Scientific, USA), and the DNA quality was observed through gel (1.2%) electrophoresis.

16S rDNA gene amplification and sequencing: The extracted DNA undergoes PCR amplification followed by high-throughput sequencing. Specific primers included forward: 5'-barcode+ACTCCTACGGGAGGCAGCA-3' and reverse: 5'-GGACTACHVGGGTWTCTAAT-3') were used for DNA amplification. Target DNA was purified from PCR amplicons by using a DNA purification kit (Axygen Biosciences, USA). After that, PCR products were quantified by using a microplate reader, and sequencing libraries were prepared by Library Prep Kit (Illumina Inc., USA) as per the manufacturer's instructions, then purified by AMPure XP beads. Validated libraries undergo high-throughput sequencing on an Illumina NovaSeq 6000 platform.

Bioinformatics and statistical analysis: Raw sequencing data were processed using QIIME2 (2023.7), and the resulting data were utilized for downstream taxonomic composition analysis. Reads were gathered into operational taxonomic units (OTUs) based on sequence similarity (97%). Differential analysis was performed using SPSS software (version 26.0, IBM, USA). Bar plots in this study were created using GraphPad Prism (version 10.0.0, GraphPad Software, USA). Bray-Curtis's distance matrix was also used for other analyses, including non-metric multi-dimensional scaling (NMDS) analysis to show microbial communities' composition differences and the Unweighted pair-group method with arithmetic (UPGMA) for clustering analysis. PICRUSt2 was used to predict gene functions based on the MetaCyc and KEGG databases, and bar charts of LDA values were generated using linear discriminant analysis effect size (LEfSe).

RESULTS

Body weight and organ index effects*:* To assess the beneficial effect of TCP therapy on LPS-induced growth retardation in mice, the average daily gain was monitored throughout the trial. From the first to the fourteenth day, the mouse's body weight steadily increases. After the LPS challenge, the weight of the mice significantly decreased; however, the decrease in TCP-treated mice was less than that in mice treated only with LPS (Fig. 1A). Moreover, TCP treatment significantly increased the spleen index decreased by LPS (Fig. 1B).

Anti-inflammatory effects: Expressions of inflammatory cytokines are a crucial indicator of inflammation. The inhibitory effects of TCP on inflammatory cytokines (IL-1β, IL-6, IL-10, and TNF-α) in LPS-treated mice were exhibited in Fig. 2A-D. The level of inflammatory cytokines was significantly increased in the LPS-challenged group compared to the control group. However, TCP treatment markedly decreased ($P<0.05$) cytokine levels compared with the LPS-challenged group.

Antioxidant effect: To detect the redox status of experimental mice, MDA, SOD, GSH-Px, and T-AOC were detected. As depicted in Fig. 2E-H, mice exposed to LPS revealed a significant increase in MDA content. Simultaneously, the activities of SOD, GSH-Px, and T-AOC were markedly ($P<0.05$) decreased as compared to the control group. Nevertheless, TCP treatment significantly ($P<0.05$) reversed LPS-induced alterations in oxidative stress markers and antioxidant enzymes in the serum of mice, as evidenced by decreased MDA content and increased SOD, GSH-Px, and T-AOC activities as compared to the LPS-challenged group.

Diversity analysis of gut microbiota: Among the C, M, and P experimental groups, over 103000, 107000, and 102000 input sequences were generated, while over 97000, 101000, and 96000 filtered sequences were generated for each sample.

Generally, the alpha-diversity index and species diversity of microbiota are positively correlated. Among the index including, including Chao1, faith_pd, Shannon, and goods_coverage, LPS-induced decrease can be observed (Fig. 3A). However, there is a significant difference in the Shannon index ($P<0.05$). Moreover, a decrease can be observed between the LPS and TCP groups, but no significant difference was detected. The rarefaction curve is also used to evaluate the sequencing saturation or sample size. Rarefaction curves of the 9 samples have all tended to be smooth and approaching the plateau period, proving that all nine bacterial community samples in this experiment are sufficient and reasonable (Fig. 3B). Curves from the control group are wider and smoother than those in the LPS and TCP groups, indicating that the species evenness of the control group is larger than the LPS and TCP groups (Fig. 3C).

Principal coordinates analysis (PCoA) based on Bray-Curtis can show the similarities or differences between microbiota community structures (Fig. 4A). The result showed that the dots in the LPS group and TCP group are more separated than the control group, indicating that the LPS and TCP groups have more obvious differences within groups. Dots in the LPS group are located more distantly than the control group, while dots in the TCP group are located beside those in the LPS group. NMDS is another

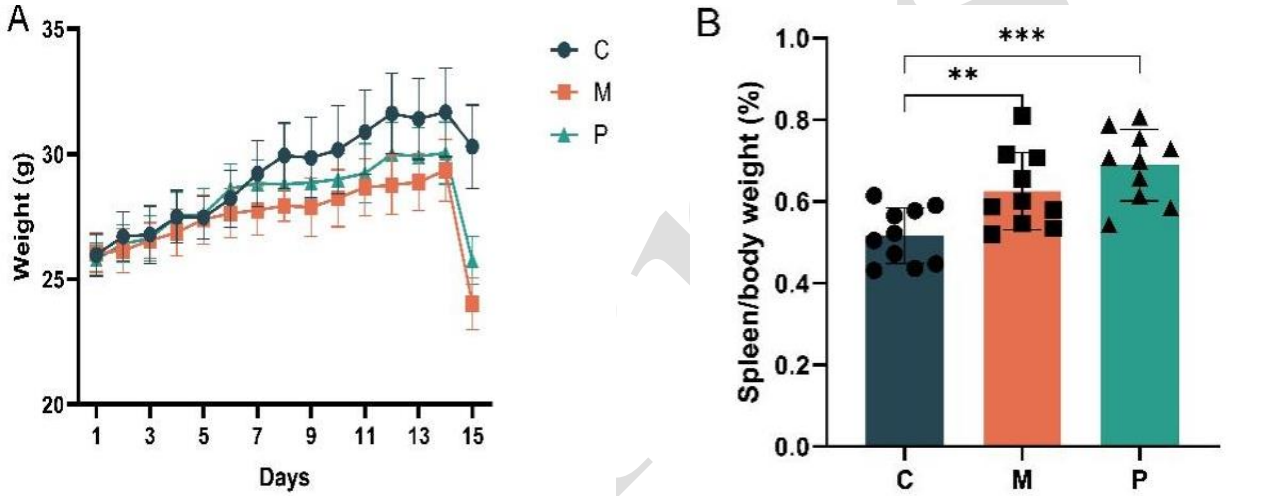

Fig. 1: The effect of *Tupistra chinensis* polysaccharides on body weight (A) and spleen index (B). ***P*<0.01, ****P*<0.001; Mean±SD.

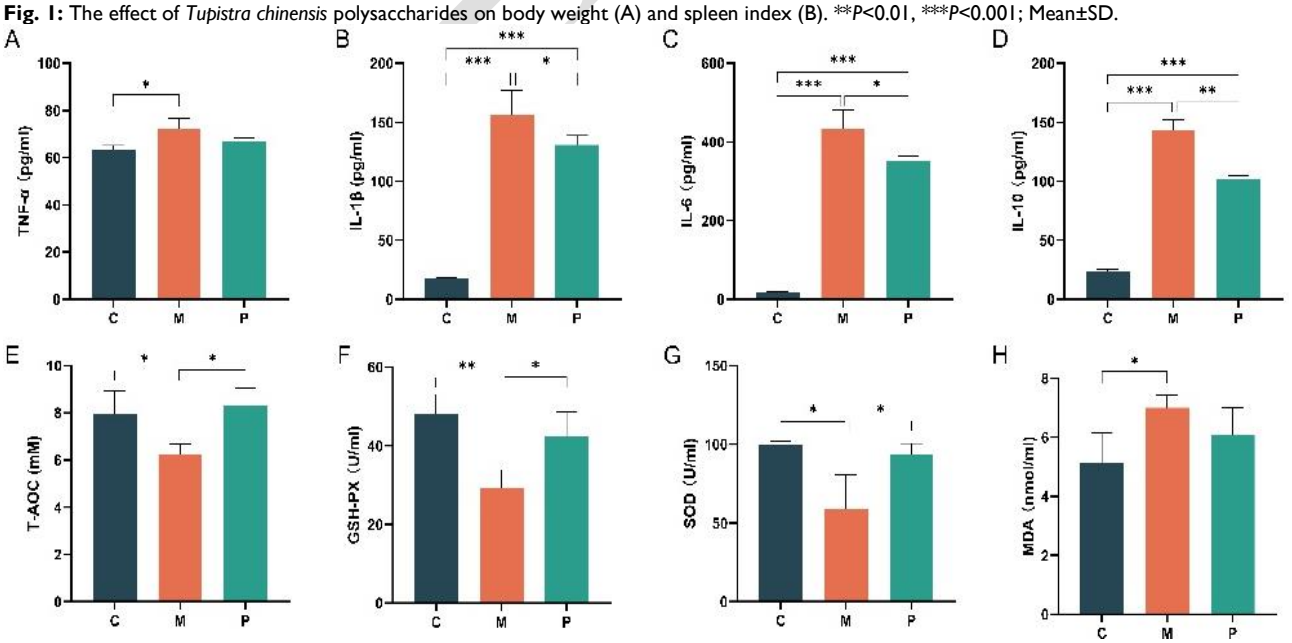

Fig. 2: The effect of TCP on cytokines and antioxidant abilities: (A) TNF-α; (B) IL-1β; (C) IL-6; (D) IL-10; (E) T-AOC; (F) GSH-px; (G) SOD, and (H) MDA. **P*<0.05, ***P*<0.01, ****P*<0.001 and *****P*<0.0001; Mean±SD.

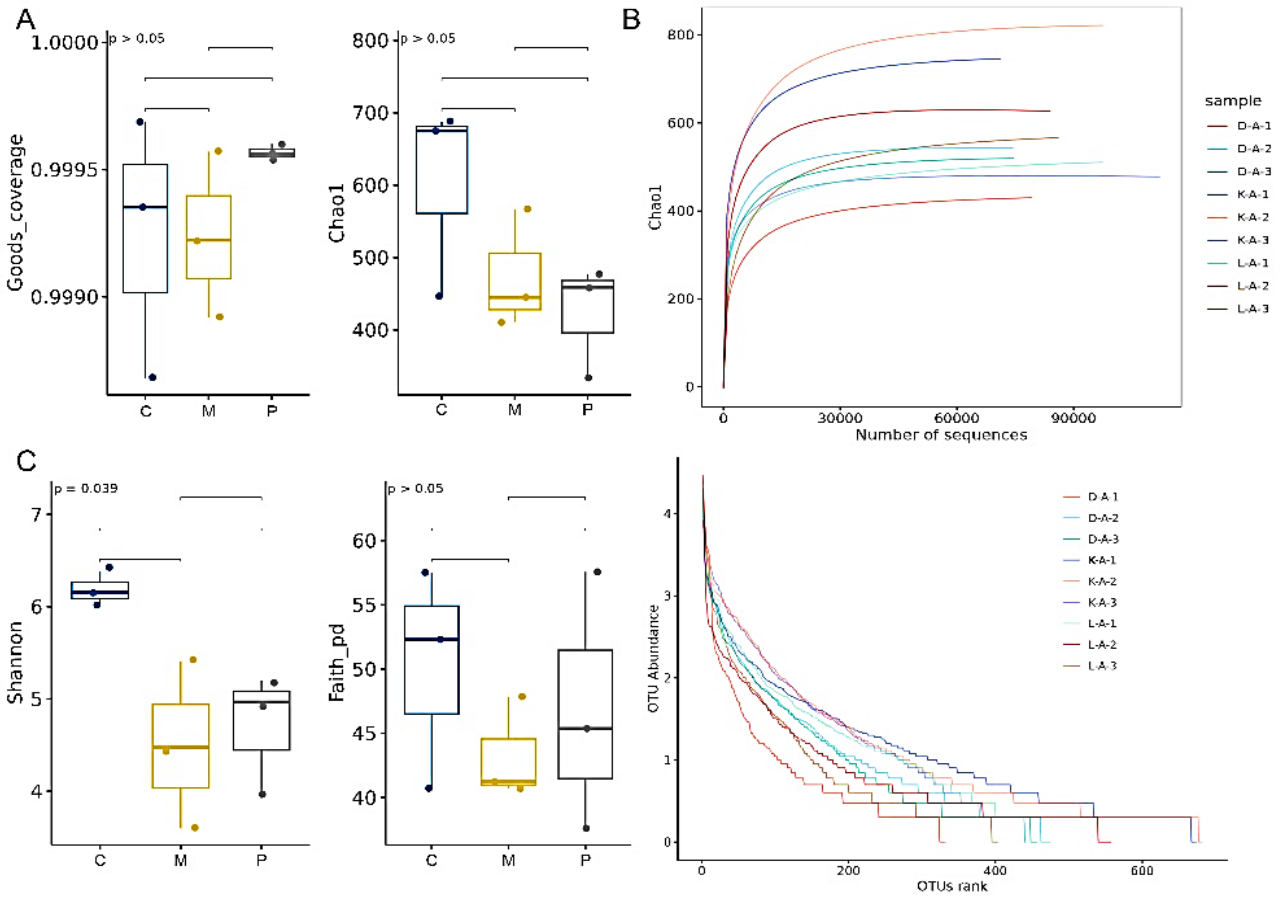

Fig. 3: Effect of *Tupistra chinensis* on alpha diversity of the gut microbiota. (A) alpha diversity index; (B) rarefaction curve; (C) rank abundance curve.

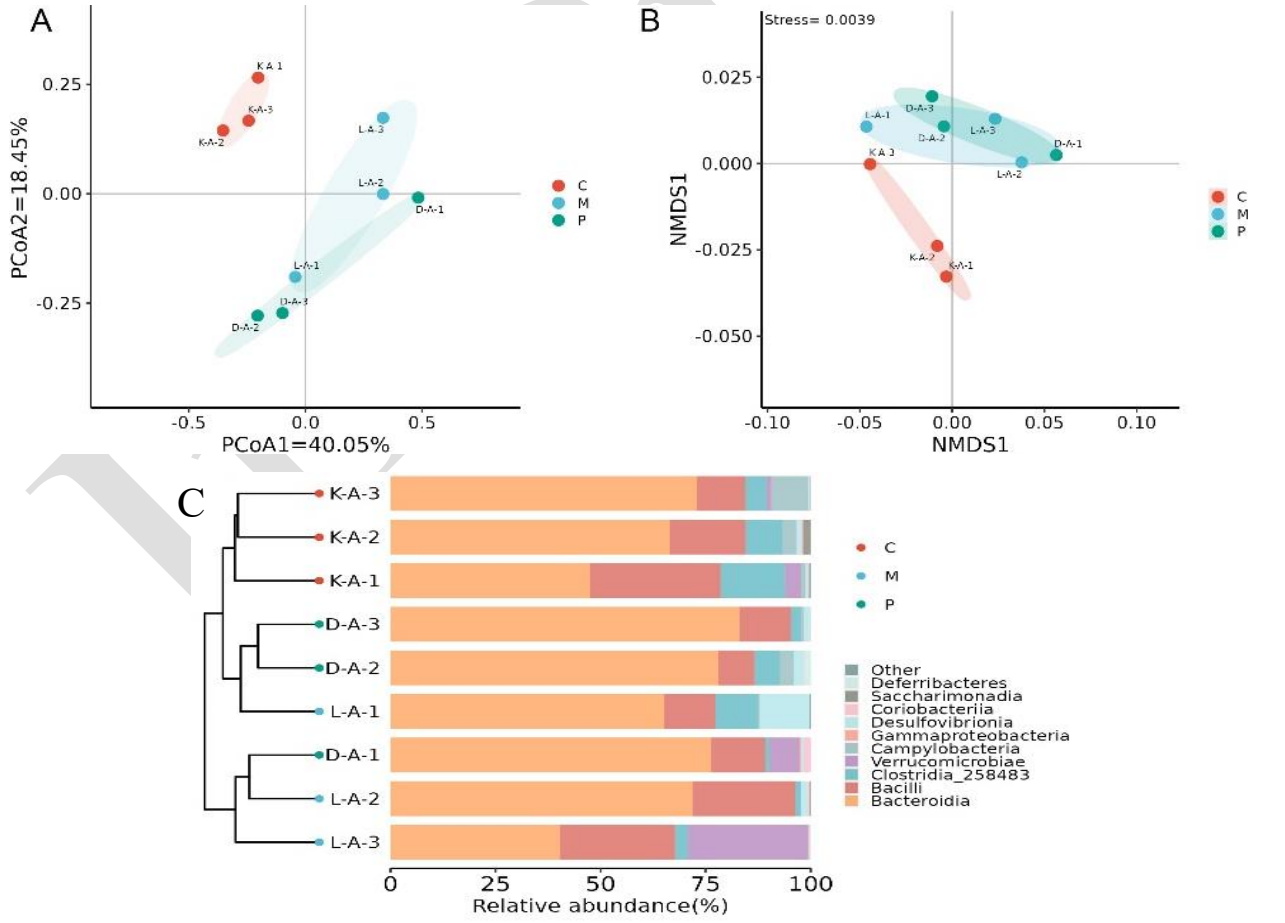

Fig. 4: Effect of *Tupistra chinensis* on beta diversity of the gut microbiota. (A) PCoA; (B) NMDS; (C) UPGMA.

kind of beta diversity analysis. Based on Bray-Curtis, the results also show that samples from the LPS and TCP groups were more separated than the control group (Fig. 4B). The UPGMA uses the classification trees to determine similarity. The classification tree between the control and the LPS group is shorter than that between the LPS group and the TCP group, revealing more similarity between the control group and the LPS group compared to the TCP group (Fig. 4C).

Composition analysis of gut microbiota: At the phylum level, *Bacteroidota* (C=62.34%, M=59.37%, P=79.11%) and *Firmicutes_D* (C=20.18%, M=21.16%, P=11.28%) were the dominant phyla. In both the control and the TCP group, the third most abundant phylum was *Firmicutes_A* (C=9.66%, P=3.21%), whereas, in the LPS group, *Verrucomicrobiota* (9.51%) occupied this position (Fig. 5A). At the class level, *Bacteroidia* (C=62.34%, M=59.37%, P=79.11%) and *Bacilli* (C=20.18%, M=21.16%, P=11.28%) were the dominant classes across all three groups. The third most abundant class in both the control and TCP groups was *Clostridia_258483* (C=9.66%, P=3.21%), whereas, in the LPS group, *Verrucomicrobiae* (9.51%) occupied this position (Fig. 5B). At the order level, *Bacteroidales* (C=62.21%, M=59.26%, P=78.92%) and *Lactobacillales* (C=19.72%, M=20.33%, P=6.08%) were the dominant orders across all groups. *Lachnospirales* (6.22%) was the third most abundant order in the control group, whereas *Verrucomicrobiales* (9.51%) occupied this position in the LPS group, and *Erysipelotrichales* (5.17%) ranked third in the TCP group (Fig. 5C). At the family level, the three most abundant families were *Muribaculaceae*, *Lactobacillaceae*, and *Bacteroidaceae*. In the control group, *Muribaculaceae* had the highest abundance (41.62%), followed by *Lactobacillaceae* (19.79%) and *Bacteroidaceae* (11.94%). In both the LPS and TCP groups, *Bacteroidaceae* was the most abundant (M=33.23%, P=48.11%), followed by *Muribaculaceae* (M=19.32%, P=24.49%) and *Lactobacillaceae* (M=19.19%, P=6.08%) (Fig. 5D). At the genus level, the three most abundant genera in the control group were *Paramuribaculum* (15.84%), *Ligilactobacillus* (11.73%), and *Duncaniella* (10.56%). Whereas in the LPS group, *Alloprevotella* (21.40%), *Akkermansia* (9.96%), and *Lactobacillus* (9.66%) were the most prevalent, while in the TCP group, *Alloprevotella* (19.92%), *Phocaeicola_A_858004* (16.59%), and *Bacteroides_H* (14.69%) occupied these positions (Fig. 5E). Furthermore, a clustering heatmap was utilized to illustrate the distribution and variability of gut microbiota at the phylum (Fig. 5F) and genus levels (Fig. 5G).

The abundance differences of bacteria at different taxa were analyzed through Student's *t*-test, and the results were plotted on bar charts. On the phylum level, the abundance of *Bacteroidota* decreased significantly after the LPS challenge and slightly increased after being treated with TCP. The abundance of *Firmicutes_D* and *Firmicutes_A* notably decreased in the LPS group, whereas their abundance showed distinct differences with TCP treatment (Fig. 6A). On the genus level, the abundance of

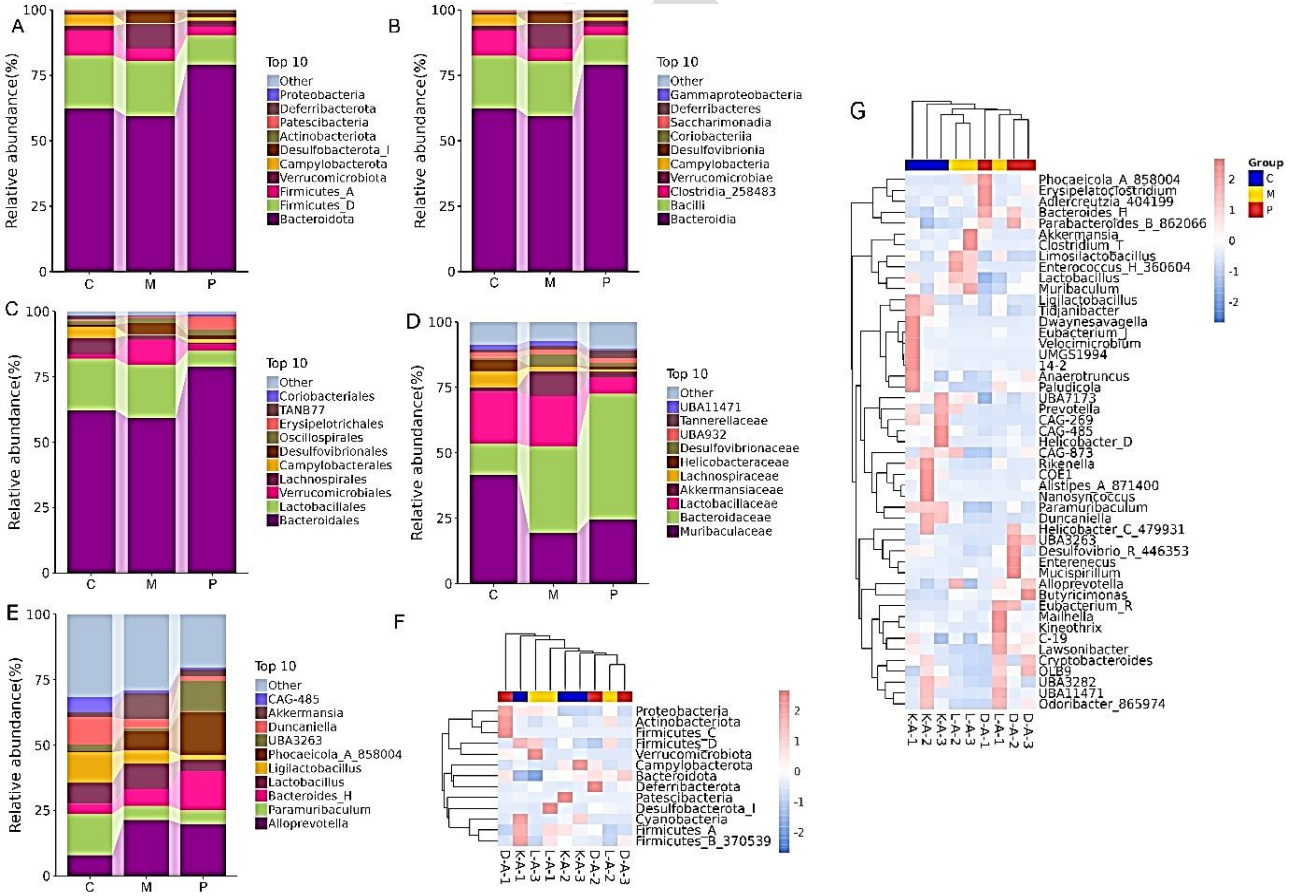

Fig. 5: The dominant bacteria and heatmap of bacterial distribution at different taxa. (A) phylum level; (B) class level; (C) order level; (D) family level; (E) genus level; (F) heatmap at phylum level; (G) heatmap at genus level.

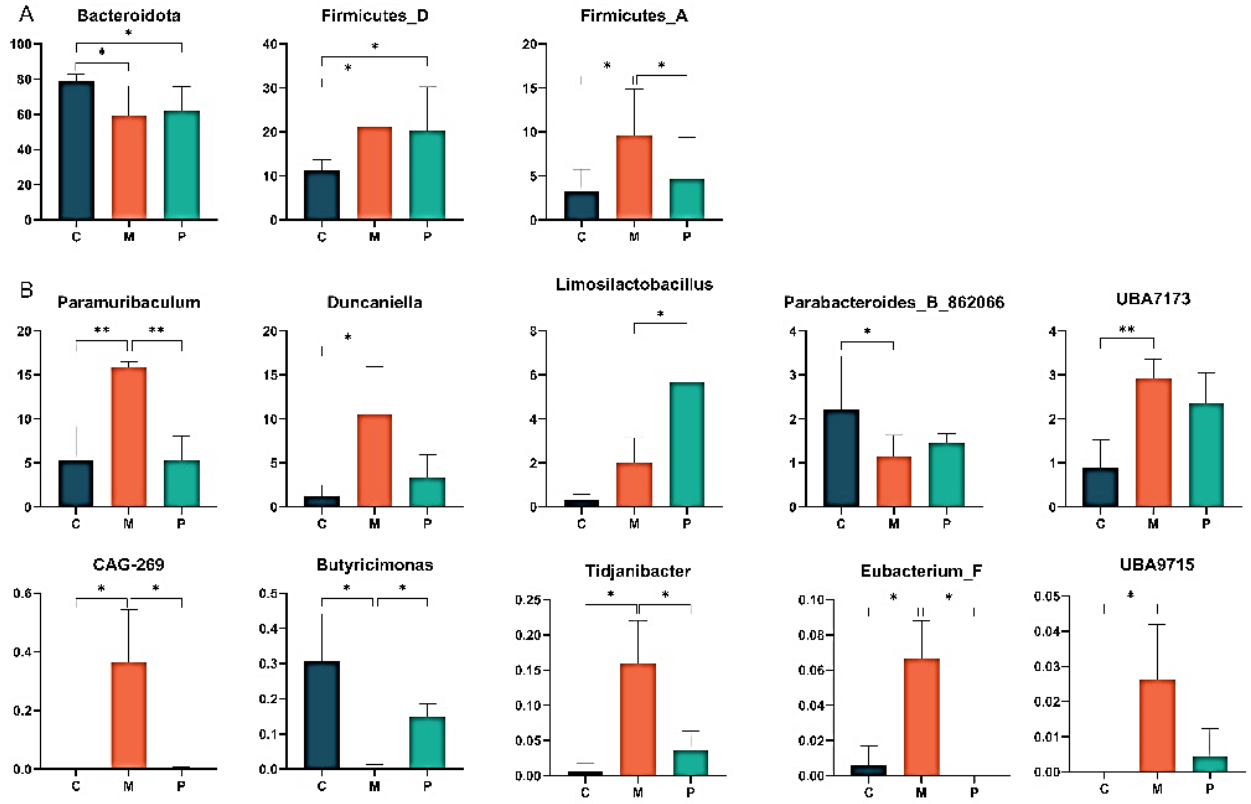

Fig. 6. *Tupistra chinensis* polysaccharide recovers the relative abundance change caused by LPS. (A) phylum level; (B) genus level. **P*<0.05, ***P*<0.01; mean ± SD.

Eubacterium_F, *Paramuribaculum*, *CAG-269*, and *Tidjanibacter* were significantly increased after LPS exposure, and significantly decreased after TCP treatment. *Duncaniella*, *Adlercreutzia_404218*, *UBA7173*, and *UBA9715* were increased, while declining at different levels. Butyricimonas and *Parabacteroides_B_862066* were notably decreased after the LPS challenge and partly recovered with TCP treatment (Fig. 6B).

TCP affects the microbiota functions of LPS-induced mice: MetaCyc is a main metabolic reference database in the field of biosciences. After fitting the distribution of OTUs and determining the significance of differences, the results were revealed in the LDA score bar chart, about various pathways in Fig. 7A. These pathways are involved in the metabolism of 5-aminoimidazole ribonucleotide, lysine, and UDP-N-acetyl-D-glucosamine. In contrast, metabolic pathways such as PWY5189 (uroporphyrinogen-III II (from glycine), AST-PWY, ORNARGDEG-PWY, ORNDEG-PWY (superpathway of ornithine degradation), ARGDEG-PWY, PWY0-1479 (tRNA processing), ENTBACSYN-PWY (enterobactin biosynthesis), PWY-6891, ALL-CHORISMATEPWY (superpathway of chorismate metabolism), were identified in the LPS group. These pathways are involved in the metabolism of arginine, ornithine, tRNA, and enterobactin, among others. KEGG is a main biological metabolic pathway analysis database. The same method was used to pare the distribution of OTUs and reveal the significance of the difference in the bar chart. Primary and secondary bile acid biosynthesis, lysine biosynthesis, and *Staphylococcus aureus* infection were also detected in the control group. Contrastingly, lysine degradation was detected in the LPS group, and histidine metabolism and peroxisomes were detected in the TCP group (Fig. 7B).

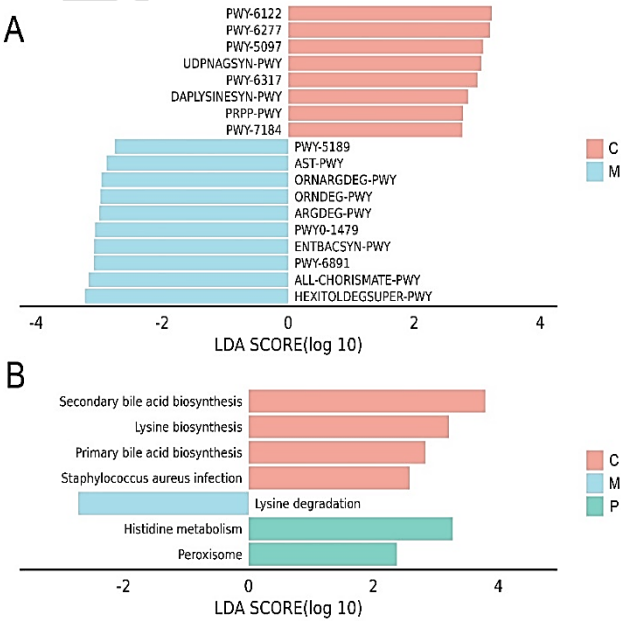

Fig. 7. TCP treatment could affect the microbiome function induced by LPS. (A) MetaCyc pathways; (B) KEGG pathways.

DISCUSSION

LPS is proven to stimulate the production of inflammation and activate the immune system (Bertani and Ruiz, 2018). Intense inflammation induced by LPS may be related to the rapid weight loss and spleen/body index

increase in mice (Yang *et al.*, 2022). Inflammatory factor levels (IL-1, IL-6, IL-10, and TNF-α) are important indicators in reflecting inflammation progress, and they are dramatically up-regulated within gut-intestinal diseases (Fonseca-Camarillo and Yamamoto-Furusho, 2015, Mao *et al.*, 2018). Our findings revealed that LPS exposure increased IL-1, IL-6, and TNF-α levels, while TCP treatment significantly decreased these contents, indicating that TCP can mitigate LPS-induced inflammatory damage. Oxidative stress is frequently caused by an imbalance of prooxidants and antioxidants, leading to gut issues and intestinal barrier dysfunction. Antioxidant enzymes like SOD and GSH-Px can resist ROS, RNS, and other free radicals (Taysi *et al.*, 2019), and the level of MDA is generally recognized as a marker of lipid peroxidation and oxidant stress (Del Rio *et al.*, 2005). In the present study, TCP treatment significantly mitigated oxidative stress by reducing MDA accumulation while improving antioxidant enzyme capacity (SOD, GSH-Px, and T-AOC) under LPS exposure. Our results agree with the previous report (Huang *et al.*, 2020) .

Studies have shown that the LPS challenge can decrease the relative abundance of *Firmicutes* and the *Firmicutes/Bacteroidota* ratio compared to the control group (Ma *et al.*, 2021). Consistent with other similar research, our study also displayed that gut microbial diversity was reduced, with significant changes observed in bacteria that might exert essential roles in intestinal homeostasis. Notably, the abundance of some genera that positively affect host health decreased after the LPS challenge, including *Bacteroidota*, *Butyricimonas*, and *Parabacteroides*. Previous studies reported that *Butyricimonas* works in the production of SCFA, and Parabacteroides contributes to the anti-inflammatory effect and maintains host-intestine homeostasis (Cui *et al.*, 2022; Su *et al.*, 2023; Wan *et al.*, 2023). In our study, there was an increasing trend of several bacteria that have negative effects on host health in the LPS-induced group, including *Adlercreutzia*, *Duncaniella*, *Eubacterium*, *Paramuribaculum*, and *Tidjanibacter*. However, TCP treatment noticeably declined their abundance. Studies have shown that alleviated *Adlercreutzia* was correlated with diabetes and insulin resistance (Deng *et al.*, 2022; Liu *et al.*, 2022). Multiple studies have proved that *Duncaniella* played an important role in inflammatory bowel disease induced by dextran sulphate sodium (Forster *et al.*, 2022). Eubacterium carries bile acid and cholesterol transformations in the gut, which is generally considered beneficial to the host, but some researchers pointed out that it was linked to obesity (Gomes *et al.*, 2018; Mukherjee *et al.*, 2020). Some evidence suggests *Paramuribaculum* was associated with DSS-induced colitis (Feng *et al*., 2022). *Tidjanibacter* was considered an opportunistic pathogen in some studies (Mailhe *et al*., 2017). Research indicates that *Tupistra chinensis* polysaccharide modulates inflammatory responses and alters gut microbiota composition. These polysaccharides downregulate pro-inflammatory cytokines, including TNF-α, IL-6, and IL-1β, and enhance anti-inflammatory mediator production (Shao *et al.,* 2023; Zhao *et al.,* 2025). They also promote beneficial gut bacteria like *Lactobacillus* while suppressing pathogenic taxa, which may improve gut barrier function and immune regulation (Sun *et al.,* 2022).

LEfSe analysis showed that *Paramuribaculum*, *Ligilactobacillus*, *Duncaniella*, and *Lactobacillus* were detected in the control group. In contrast, *Alloprevotella*, *Akkermansia*, *Lactobacillus*, and *Phocaeicola* were detected in the LPS group, and *Alloprevotella*, *Phocaeicola*, *Bacteroides,* and *UBA3263* were detected in the TCP group. *Ligilactobacillus* is a good probiotic for its contributions to metabolism and regulation, not only in the gut but also in the oral cavity, lungs, and vagina (Chuandong *et al.*, 2024; Yang *et al.*, 2024). *Alloprevotella* was closely related to methylacetic metabolism, but it was generally considered an opportunistic pathogen; its abundance can be remarkably linked to various diseases, including obesity, chronic kidney diseases, and even cancer (Li *et al.*, 2019; Zhang *et al.*, 2019). Compared to the LPS group, the relative abundance of *Phocaeicola* in the TCP group was increased, showing a positive correlation with unconjugated bile acids. This increase in abundance can mitigate the development of metabolic dysfunction-associated steatotic liver disease (MAFLD) (Jin *et al.*, 2024). Several studies have reported that *UBA3263* is from the family Muribaculaceae, which has been linked to the alleviation of Ulcerative colitis (Wu *et al.*, 2023).

Conclusions: Our results showed that LPS challenge can lead to gut microbiota disruption, antioxidant capacity, and inflammation. However, *Tupistra chinensis* polysaccharide could reverse the negative effects from LPS challenge and regulate gut microbiota and antioxidant capacity.

Data availability statement: The raw data in this study were deposited in the NCBI database under accession number: PRJNA1104810.

Author contributions: KL and XL, research idea and methodology. XL, JDC, CX, and QH, reagents, materials, and analysis tools. JDC, CX, XL, MA, KL, and XL writing the original draft and preparation. KL, writing-review and editing. KL, visualization, and supervision. All authors have read and agreed to the published version of the manuscript.

Funding: This research was funded by the Innovation Capability Enhancement Project of Technology-based Small and Medium-sized Enterprises of Shandong Province (2023TSGC0235).

REFERENCES

Anjum FR, Anam S, Rahman SU, *et al*., 2020. Anti-chicken type I IFN countermeasures by major avian RNA viruses. Virus Res 286:198061.

Bertani B and Ruiz N, 2018. Function and Biogenesis of Lipopolysaccharides. EcoSal Plus 8(1): 10.

Buffie CG, Bucci V, Stein RR, *et al*., 2015. Precision microbiome reconstitution restores bile acid mediated resistance to *Clostridium difficile*. Nature 517(7533): 205-8.

Chuandong Z, Hu J, Li J, *et al*., 2024. Distribution and roles of *Ligilactobacillus murinus* in hosts. Microbiol Res 282: 127648.

Cui Y, Zhang L, Wang X, *et al*., 2022. Roles of intestinal *Parabacteroides* in human health and diseases. FEMS Microbiol Lett 369(1): fnac072.

Del Rio D, Stewart AJ and Pellegrini N, 2005. A review of recent studies on malondialdehyde as toxic molecule and biological marker of oxidative stress. Nutr Metab Cardiovas Dis 15(4): 316-28.

Deng K, Shuai M, Zhang Z, *et al*., 2022. Temporal relationship among adiposity, gut microbiota, and insulin resistance in a longitudinal human cohort. BMC Med 20(1): 171.

Fan Y and Pedersen O, 2021. Gut microbiota in human metabolic health and disease. Nat Rev Microbiol 19(1): 55-71.

Feng P, Li Q, Liu L, *et al.*, 2022. Crocetin prolongs recovery period of DSS-Induced Colitis via altering intestinal microbiome and increasing intestinal permeability. Int J Mol Sci 23(7): 3832.

Fonseca-Camarillo G and Yamamoto-Furusho JK, 2015. Immunoregulatory pathways involved in inflammatory bowel disease. Inflamm Bowel Dis 21(9): 2188-93.

Forster SC, Clare S, Beresford-Jones BS, *et al.*, 2022. Identification of gut microbial species linked with disease variability in a widely used mouse model of colitis. Nat Microbiol 7(4): 590-9.

Gomes AC, Hoffmann C and Mota JF, 2018. The human gut microbiota: metabolism and perspective in obesity. Gut Microbes 9(4): 308-25.

He Y, Xu M, Lu S, *et al.*, 2023. Seaweed polysaccharides treatment alleviates injury of inflammatory responses and gut barrier in LPS-induced mice. Microb Pathog 180: 106159.

Hong H, Lou S, Zheng F, *et al.*, 2022. Hydnocarpin D attenuates lipopolysaccharide-induced acute lung injury via MAPK/NF-kappaB and Keap1/Nrf2/HO-1 pathway. Phytomedicine 101: 154143.

Huang CY, Deng JS, Huang WC, *et al.*, 2020. Attenuation of lipopolysaccharide-induced acute lung injury by hispolon in mice, through regulating the TLR4/PI3K/Akt/mTOR and Keap1/Nrf2/HO-1 pathways, and suppressing oxidative stress-mediated er stress-induced apoptosis and autophagy. Nutrients 12(6): 1742.

Huang W, 2013. Anticancer effect of plant-derived polysaccharides on mice. J Cancer Ther, 4(2): 500-3.

Jin S, Chen P, Yang J, *et al.*, 2024. *Phocaeicola vulgatus* alleviates diet-induced metabolic dysfunction-associated steatotic liver disease progression by downregulating histone acetylation level via 3-HPAA. Gut Microb 16(1): 2309683.

Kesika P, Suganthy N, Sivamaruthi BS, *et al.*, 2021. Role of gut-brain axis, gut microbial composition, and probiotic intervention in Alzheimer's disease. Life Sci: 264: 118627.

Li F, Wang M, Wang J, *et al.*, 2019. Alterations to the gut microbiota and their correlation with inflammatory factors in chronic kidney disease. Front Cell Infect Microbiol 9: 206.

Li Y, Wang X, He H, *et al.*, 2015. Steroidal saponins from the roots and rhizomes of *Tupistra chinensis*. Molecules 20(8): 13659-69.

Liu K, Zou J, Fan H, *et al.*, 2022. Causal effects of gut microbiota on diabetic retinopathy: a Mendelian randomization study. Front Immunol 13: 930318.

Ma Y, Liu G, Tang MY, *et al.*, 2021. Epigallocatechin gallate can protect mice from acute stress induced by LPS while stabilizing gut microbes and serum metabolites levels. Front Immunol 12: 640305.

Mailhe M, Ricaboni D, Benezech A, *et al.*, 2017. '*Tidjanibacter massiliensis*' gen. nov., sp. nov., a new bacterial species isolated from human colon. New Microbes New Infect 17: 21-2.

Mao L, Kitani A, Strober W, *et al.*, 2018. The role of NLRP3 and IL-1beta in the pathogenesis of inflammatory bowel disease. Front Immunol 9: 2566.

Marchesi JR, Adams DH, Fava F, *et al.*, 2016. The gut microbiota and host health: a new clinical frontier. Gut 65(2): 330-9.

Mukherjee A, Lordan C, Ross RP, *et al.*, 2020. Gut microbes from the phylogenetically diverse genus *Eubacterium* and their various contributions to gut health. Gut Microbes 12(1): 1802866.

Pan ZH, Li Y, Liu JL, *et al.*, 2012. A cytotoxic cardenolide and a saponin from the rhizomes of *Tupistra chinensis*. Fitoterapia 83(8): 1489-93.

Qian K, Tan T, Ouyang H, *et al.*, 2020. Structural characterization of a homopolysaccharide with hypoglycemic activity from the roots of *Pueraria lobata*. Food Funct 11(8): 7104-14.

Rai P, Chakraborty M, Chutia D, *et al.*, 2024. Unveiling the therapeutical potential of *Tupistra clarkei* in diabetic neuropathic pain on Wistar albino rats: A Himalayan Gem. Pharmac Res-Nat Prod 5:100092.

Sassone-Corsi M, Nuccio SP, Liu H, *et al.*, 2016. Microcins mediate competition among Enterobacteriaceae in the inflamed gut. Nature 540(7632): 280-3.

Shao X, Li J, Zhang H, *et al.*, 2023. Anti-inflammatory effects and molecular mechanisms of bioactive small molecule garlic polysaccharide. Front Nut 9:1092873.

Si HF, Yang Q, Hu H, *et al.*, 2021. Colorectal cancer occurrence and treatment based on changes in intestinal flora. Semin Cancer Biol 70: 3-10.

Song B, Huang W, Li Y, *et al.*, 2021. Three new steroidal saponins from the roots and rhizomes of Rohdea chinensis (Baker) N.Tanaka (synonym Tupistra chinensis Baker). Nat Prod Res 35(1): 108-15.

Song WS, Hung TH, Liu SH, *et al.*, 2023. Neuroprotection by abdominal ultrasound in lipopolysaccharide-induced systemic inflammation. Int J Mol Sci 24(11):9329.

Su Q, Tun HM, Liu Q, *et al.*, 2023. Gut microbiome signatures reflect different subtypes of irritable bowel syndrome. Gut Microbes 15(1): 2157697.

Sun Y, Ho CT, Zhang Y, *et al.*, 2022. Plant polysaccharides utilized by gut microbiota: New players in ameliorating cognitive impairment. J Tradit Complement Med13(2):128-134.

Taysi S, Tascan AS, Ugur MG, *et al.*, 2019. Radicals, oxidative/nitrosative stress and preeclampsia. Mini Rev Med Chem 19(3): 178-93.

Wan W, Qiu Y, Huang X, *et al.*, 2023. Causal relationship between *Butyricimonas* and allergic asthma: a two-sample Mendelian randomization study. Front Microbiol 14: 1190765.

Wang FL, Ji YB and Yang B, 2020a. Sulfated modification, characterization and monosaccharide composition analysis of *Undaria pinnatifida* polysaccharides and anti-tumor activity. Exp Ther Med 20(1): 630-6.

Wang Y, Xiang L, Wang Z, *et al.*, 2020b. New anti-neuroinflammatory steroids against LPS-induced NO production in BV2 microglia cells by microbial transformation of isorhodeasapogenin. Bioorg Chem 101: 103870.

Wilson ID and Nicholson JK, 2017. Gut microbiome interactions with drug metabolism, efficacy, and toxicity. Transl Res 179: 204-22.

Wu H, Tremaroli V, Schmidt C, *et al.*, 2020. The gut microbiota in prediabetes and diabetes: a population-based cross-sectional study. Cell Metab 32(3): 379–390.e3

Wu Y, Ran L, Yang Y, *et al.*, 2023. Deferasirox alleviates DSS-induced ulcerative colitis in mice by inhibiting ferroptosis and improving intestinal microbiota. Life Sci 314: 121312.

Xu J, Wang Z, Huang Y, *et al.*, 2020. A spirostanol saponin isolated from *Tupistra chinensis* Baker simultaneously induces apoptosis and autophagy by regulating the JNK pathway in human gastric cancer cells. Steroids 164: 108737.

Yang L, Wu G, Wu Q, *et al.*, 2022. METTL3 overexpression aggravates LPS-induced cellular inflammation in mouse intestinal epithelial cells and DSS-induced IBD in mice. Cell Death Discov 8(1): 62.

Yang Y, Song X, Wang G, *et al.*, 2024. Understanding *Ligilactobacillus salivarius* from probiotic properties to omics technology: a review. Foods 13(6): 895.

Zhang L, Liu Y, Zheng HJ, *et al.*, 2019. The oral microbiota may have influence on oral cancer. Front Cell Infect Microbiol 9: 476.

Zhang Y, Li X, Luo Z, *et al.*, 2020. ECM1 is an essential factor for the determination of M1 macrophage polarization in IBD in response to LPS stimulation. Proc Natl Acad Sci U S A 117(6): 3083-92.

Zhao T, Wang C, Liu Y, *et al.*, 2025. The role of polysaccharides in immune regulation through gut microbiota: mechanisms and implications. Front Immunol 16:1555414.

Zhou CD, Hu JC, Li JW, *et al.*, 2024. Distribution and roles of *Ligilactobacillus murinus* in hosts. Microb Res 282: 127648.